High sensitivity and high selectivity terahertz biomedical imaging

(Invited Paper)

Seongsin M. Kim*, William Baughman, David S. Wilbert, Lee Butler, Michael Bolus, Soner Balci, and Patrick Kung

Department of Electrical and Computer Engineering, University of Alabama, Tuscaloosa, Alabama 35487, USA

**Corresponding author: seongsin@eng.ua.edu*

Received July 4, 2011; accepted July 28, 2011; posted online September 30, 2011

We demonstrate two distinct emerging terahertz (THz) biomedical imaging techniques. One is based on the use of a new single frequency THz quantum cascade laser and the other is based on broadband THz time domain spectrocopy. The first method is employed to derive a metastasis lung tissue imaging at 3.7 THz with clear contrast between cancerous and healthy areas. The second approach is used to study an osseous tissue under several imaging modalities and achieve full THz spectroscopic imaging based on the frequency domain or on a fixed THz propagation time-delay. Sufficient contrast is achieved which facilitated the identification of regions with different cellular types and density compositions.

OCIS codes: 110.0110, 100.0100, 170.0170.
doi: 10.3788/COL201109.110009.

Terahertz (THz) imaging is a non-destructive, non-ionizing imaging technology with potential applications in medicine, dentistry, pharmaceuticals, and homeland security[1−5]. In these applications, THz biomedical imaging has become a particularly important and active field of research because of the potential for safer early screening of a disease. This will benefit the medical community tremendously and create considerable sociological impact.

THz radiation encompasses a range of frequencies in the electromagnetic spectrum between 300 GHz and 10 THz. THz radiation has the unique ability to penetrate safely a wide variety of non-conducting materials, including cloth, paper, cardboard, wood, and plastic. In addition, it is non-ionizing and its sub-mm wavelength not only makes high-resolution medical imaging possible but also has the capability to yield biologically meaningful information. This capability is the result of numerous important molecular vibrational frequencies that occur in the THz region, a largely underdeveloped region. Based on these, THz biomedical imaging is expected to complement current imaging techniques for disease screening, such as X-rays, ultrasound, and magnetic resonance imaging, by enabling a better resolution, higher specificity, and better safety. Investigations on several applications of THz waves in medicine including those for skin and breast cancers as well as dentistry and osteoarthritis have increased in recent years[6,7]. However, all methods remain strongly dependent on THz sources and detectors used.

THz time-domain spectroscopy (TDS) is one of the most successful techniques in terms of generating and detecting THz radiation without the need for cryogenic cooling. It also enables access to both the amplitude and phase information of the traveling THz waves. As a result of the direct time resolved detection method for the THz electric field, unique spectroscopic information on the imaged objects can be extracted from the TDS measurements. In addition, THz TDS is capable of yielding imaging contrast at different THz frequencies. This spectroscopic capability is considered a unique feature of THz imaging and can be very useful for both screening and diagnostics in biomedical imaging.

This is in contrast to a single frequency THz imaging, which is another possible imaging modality. Recent technological advances in quantum cascade lasers (QCLs) have enabled the application of QCLs in the generation of THz radiation over a range of useful individual frequencies[8]. Even though it remains limited to low temperature operation, the potential compact and cost-effective system based on high power QCLs will bring significant advantages in medical imaging over conventional techniques to generate THz waves, which require bulky and expensive femtosecond lasers. QCLs also have the additional benefit of coherence compared to other sources, which enables coherent detection.

In this letter, we report on THz imaging of biological tissues using two distinct methods of imaging, namely, the single frequency THz QCL and the THz TDS system.

The single frequency imaging setup consists of a QCL emitting at 3.7 THz and mounted on a cryostat cooled down to 28 K, a helium-cooled germanium bolometer, and motion controlled stages. The detailed setup has been reported in an earlier study[5]. An off-axis parabolic mirror collects the emission from the THz QCL, which is subsequently focused and transmitted through a polypropylene hyperboloidal window. The laser beam divergence angle is approximately 25° and a 7.5-cm-diameter off-axis mirror is used to minimize loss. The collimated THz radiation is focused by another off-axis mirror onto the sample. The latter is mounted on a computer controlled $x-y$ translational stage and moves in the plane perpendicular to the optic axis. The sample holder is designed to be transparent to the laser beam and thus, tissues can be safely fixed on it. The THz beam transmitted through the sample is collimated again and refocused onto a helium-cooled germanium bolometer. The THz QCL is operated with a pulse width of 300 ns

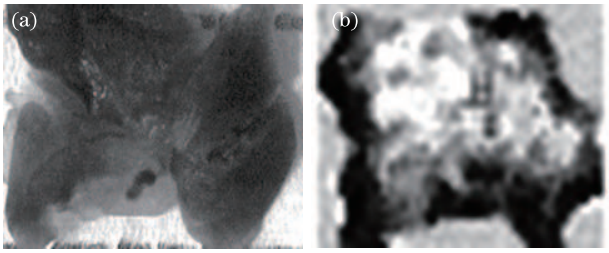

Fig. 1. (a) Optical photograph and (b) THz image of a lung tissue. Sample size is 12×10×2 (mm). THz image consists of 1 400 pixels. For THz images, the lowest transmission is indicated by black, whereas the highest transmission is indicated by white.

and a repetition rate of 1 kHz, which match closely with the frequency response of the Ge bolometer. The peak output power of the laser is 4 mW, which is converted to a pulse energy of approximately 1.2 nJ.

Figure 1 shows both optical and THz images of a metastasis lung tissue obtained at 3.7 THz ($\lambda = 81$ μm). The sample size was 12×10 (mm) and the THz images consists of 1 400 pixels with 300 μm spacing between each pixel. The spacing was set based on the tightly focused THz beam size in our imaging system (280 μm). The tissue was incised from a mouse, fixed in formalin, and sliced to a thickness of 2 mm. The samples were not dehydrated in alcohol but air dried right before scanning to ensure that the natural levels of water content are left in the structures during THz imaging[9]. The tumors were fully developed and resulted in inhomogeneous tissue densities that led to an observable contrast during the conduct of THz transmission imaging. Because tumors generally contain more water and less fat, they appear as darker areas.

The second THz imaging method was conducted on an osseous tissue and was based on THz TDS. One of the promising application of THz imaging is early detection and indication of bone disease. Osteoarthritis (OA) is the most common form of arthritis which is caused by the breakdown of cartilage. According to a National Institutes of Health (NIH) report, almost 20% of men and women aged over 60 have symptomatic OA. Another major concern for elderly people is osteoporosis (OP) or the decrease in bone density with age that can lead to increased risk of fracture, a critical condition for the elderly. Early detection of OA or OP and the subsequent prevention for retardation and damage on subchondral bone are crucial to measures aimed at decreasing the occurrence of fatal accidents. In current clinics, no guidance or method for screening and early detection exists. Electromagnetic waves in the THz region interact with materials at the molecular level. Thus, cellular structures and structural properties of tissues can be uniquely characterized while their compositions can be identified. The results can be used for early recognition of the degradation of any osseous tissues. For example, THz reflection imaging has been used successfully to determine the thickness of joint cartilage with various degrees of OA[10]. However, full spectrum THz imaging has not been fully investigated.

In this letter, we studied THz imaging in a THz transmission mode of a thin cross-section of tissue taken from the distal epiphysis of a chicken femur. The epiphysis was chosen to include both osseous tissue and articular cartilage[11]. Our THz TDS system is based on a mode-locked Ti:sapphire ultrafast laser which emits 120-fs pulses at a wavelength of 780 nm with an average power of 120 mW. The pulses are split into pump and probe beams. The pump beam is focused onto a low-temperature grown GaAs (LT-GaAs) photoconductive antenna integrated with a silicon lens while a high voltage bias is pulsed across the antenna to emit the THz radiation. The probe beam is guided via a delay line to detect the THz radiation through the electro-optics sampling based on ZnTe. This is shown in Fig. 2. The resulting THz signal pulse width is approximately 0.5 ps.

The studied bone tissue (Fig. 3(a)) was fixed on a specially designed sample holder mounted on a triple-axis motion controlled stage and raster-scanned in the focal plane normal to the propagation direction of the focused THz beam as described in Fig. 2. To calibrate the imaging system, the sample and stage were positioned in a manner where only one known type of tissue was in the path of the propagation at a time. Calibration time delayed waveforms corresponding to the THz wave transmitted through each known tissue type were

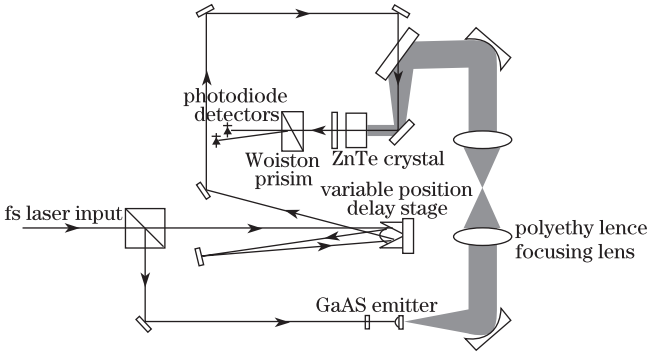

Fig. 2. Schematic diagram of the THz TDS imaging system setup.

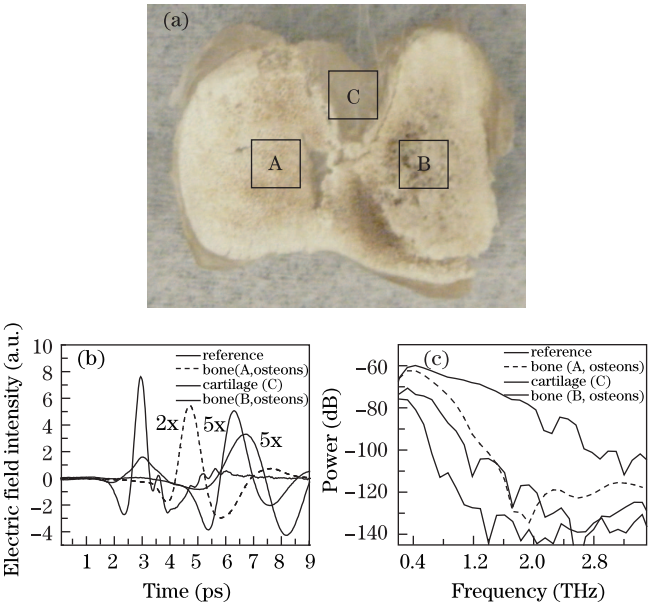

Fig. 3. (a) Photograph of distal epiphysis of a chicken femur, (b) THz time domain signal transmitted through the tissue, (c) THz power spectra obtained from FFT of signal in (b).

recorded, which allowed for the determination of the THz pulse width and peak intensities. Figures 3(b) and (c) show the THz response obtained from three distinct calibration areas of the bone tissue, namely, (A) regular spongy bone, (B) area where the osteocytes are seen, and (C) articular cartilage. Each calibration site is indicated on the photograph of the bone tissue in Fig. 3(a). Figure 3(b) plots the electric field intensity of the transmitted THz wave as a function of time delay between the pump and probe beam in comparison with the reference beam (i.e., transmitted through free space). Figure 3(c) plots the power spectra of the transmitted THz wave as a function of frequency, which were obtained by conducting the fast Fourier transform (FFT) of the electric field intensity in Fig. 3(b).

As shown in Fig. 3(b), significant changes in the THz waveform occurred not only in the signal strength but also in the time delay, indicating that each site has relatively different physical properties in addition to their absorptive nature. For example, the THz signal at area (B) is strongly attenuated and broadened by more than 4 ps in time compared with the response at area (A), which corresponds to a phase change in the THz wave. This phase change is attributed to the differences in the properties of the media encountered by the THz wave even with the use of the same bone tissue. In our experiments, thickness variation is not likely to account for this increased delay because thickness variations across the sample were minimized during the preparation and with the use of a sample holder that can exert equal pressure on the tissue.

The power spectra in Fig. 3(c) clearly show several characteristic absorption peaks at specific frequencies. The cartilage area (C) shows a strong absorption at 1.18 and 1.67 THz, whereas for the bone area, only area (B) shows distinct absorption peaks at 0.75, 1.07, and 1.39 THz.

Subsequent to the calibration measurements, the bone tissue was scanned in the focal plane normal to the propagation direction of the focused THz beam and similar transmitted THz waveforms were obtained for each pixel in a 50×40 (pixel) array corresponding to a physical sample size of 20×16 (mm). The pixel pitch was 400 μm. The full time domain signal waveform was recorded for each pixel, which was then used in post-measurement data processing to reconstruct contrast images and extract meaningful information on the material probed. Figure 4(a) is an example of THz image that can be obtained by associating the peak electric field intensity (maximum value from the waveforms such as those shown in Fig. 3(b)) to each pixel. The difference obtained from the highest intensity values yields the observed contrast. The resulting image is shown in grayscale. White color indicates higher intensity and black indicates lower intensity of the transmitted THz electric field. As shown in the image, areas (A) and (B) exhibit different contrasts and intensities, which correspond with the calibration transmission curves shown in Fig. 3(b). Area (A) has higher THz transmission. For areas (B) and (C), no significant difference in the peak electric field intensity values can be found, which did not lead to good contrast between the areas even though they contained two very different types of tissue and their transmission waveforms clearly showed very different signal delays and broadening.

Better contrast can be obtained by considering the power frequency domain spectra. Figures 4(b)–(e) shows another example of the THz image mode in which contrast is achieved by taking the value of the transmitted power at a specific frequency from the power spectra at each pixel, similar to those shown in Fig. 3(c). Four different images are presented, corresponding to four chosen fixed frequencies, namely, 0.3, 0.5, 0.7, and 1.0 THz. Because each pixel has a different frequency spectrum, the power at different frequencies yields different contrasts from the peak time-domain values previously considered. In fact, areas (B) and (C) show dramatic contrast changes from 0.3 to 0.5 THz. Furthermore, the cartilage (area (C)) that apparently appears uniform at 0.3 THz reveals more interesting features at 0.5 THz. Such spectroscopic imaging is a unique capability of a THz TDS system, which the single frequency THz imaging used for Fig. 1 cannot realize. The ability to carry out spectroscopic imaging can be useful in detecting and enhancing the contrast of an area of interest without the use of contrast agents.

Further imaging contrast can also be achieved by introducing the parameter of time delay in the transmitted THz wave (in the order of a few picoseconds) which is one of the most important information that can be obtained through spectroscopic imaging. The delay occurs

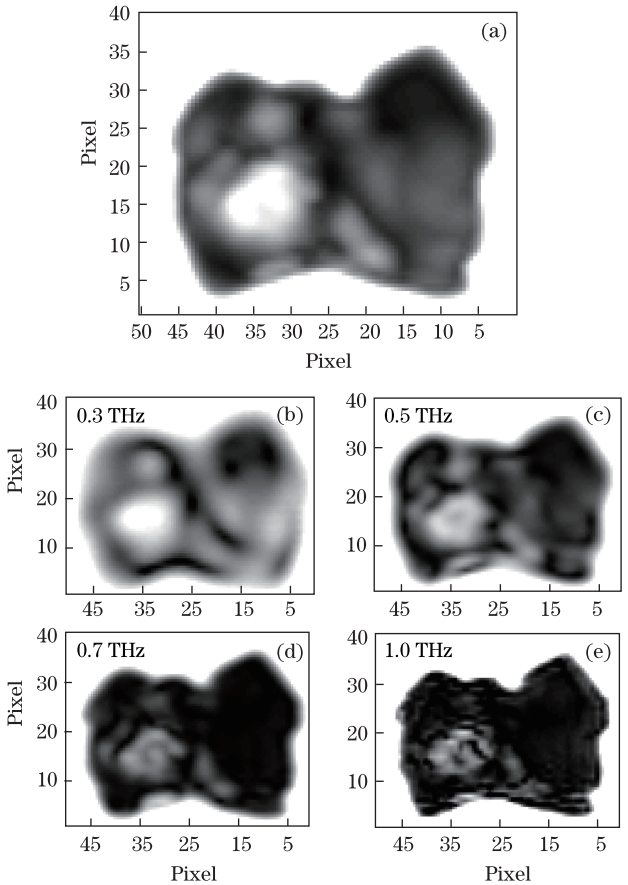

Fig. 4. (a) THz image of bone tissue with 50×40 (pixels). Image is based on the peak intensity of the time-domain signal, (b)–(e) reconstructed THz images based on power spectra. Each pixel is obtained from FFT of the time domain signal, which is reconstructed at fixed frequencies.

due to the combination of absorbance, dielectric properties, density, and thickness of the sample probed. As the thickness was maintained uniform in the experiments, what was observed in the different delay properties of each pixel can be related directly to the structural and physical properties of each point of the samples. To take full advantage of this feature, we developed a fixed delay analysis approach, which polls the intensities of the transmitted electric field (such as those in Fig. 3(b)) at a chosen fixed value of time delay for all pixels. Examples of reconstructed images obtained at several fixed delays are shown in Fig. 5. The THz TDS system achieves a time delay by physically moving a mirror which extends the propagation path of the probe laser beam. This is the reason for the ease of referring to a time delay in terms of distance delay. In the images in Fig. 5, a position delay of 25.8 mm corresponds to zero time, whereas a 26.5-mm position delay corresponds to 9 ps. Figure 5 shows that very high contrast images of the bone tissue can be obtained by adjusting the delayed distances from 26.060 to 26.366 mm. Although the current tissue sample is limited and cannot be probed for direct structural and physiological information, the spectroscopic THz imaging shows great potential for multimodal imaging that enriches the information from the each pixel.

In conclusion, we present and apply two distinct THz biomedical imaging techniques. One is based on the transmission of THz radiation generated from a single frequency (3.7 THz) cryogenically operated QCL and the other is based on a room temperature THz TDS system. We achieve a clear indication of cancerous regions in metastasis lung tissue imaged at 3.7 THz using the first technique and successfully demonstrate the powerful spectroscopic imaging capability of the second technique for osseous tissues.

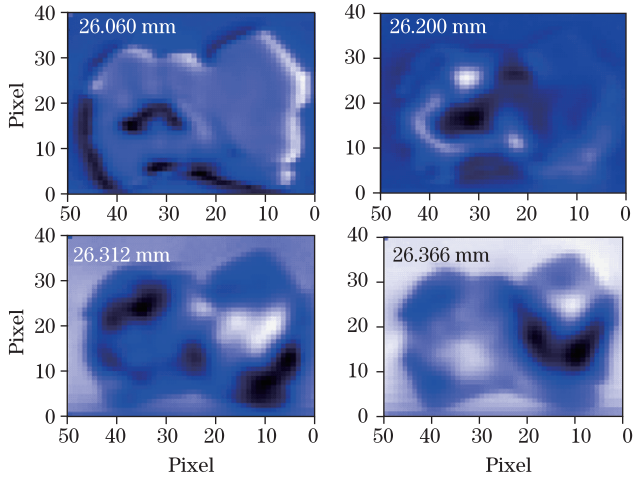

Fig. 5. Reconstructed images obtained at several fixed delays.

Soner Balci acknowledges the support of the Turkish National Scholarship. This work was supported by the National Science Foundation, USA.

References

1. R. M. Woodward, V. P. Wallace, R. J. Pye, B. E. Cole, D. D. Arnone, E. H. Linfield, and M. Pepper, J. Invest. Dermatol. **120,** 72 (2003).
2. A. J. Fitzgerald, V. P. Wallace, M. Jimenez-Linan, L. Bobrow, E. J. Pye, A. D. Purushotham, and D. D. Arnone, Radiology **239,** 533 (2006).
3. D. Crawley, C. Longbottom, B. E. Cole, C. M. Ciesla, D. Arnone, V. P. Wallace, and M. Pepper, CariesRes. **37,** 352 (2003).
4. C. J. Strachan, P. F. Taddy, and D. A. Newnham, J. Pharm. Sci. **94,** 837 (2005).
5. S. M. Kim, F. Hatami, A. W. Kurian, D. King, J. Ford, J. S. Harris, G. Scalari, M. Giovannini, N. Hoyler, J. Faist, and G. S. Harris, Appl. Phys. Lett. **88,** 153903 (2006).
6. M. R. Stringer, D. N. Lund, A. P. Foulds, A. Uddin, E. Berry, R. E. Miles, and A. G. Davies, J. Phys. Med. Biol. **50,** 3211 (2005).
7. R. M. Woodward, B. E. Cole, V. P. Wallace, R. J. Pye, D. D. Arnone, E. Linfield, and M. Pepper, J. Phys. Med. Biol. **47,** 3853 (2002).
8. S. Kumar, B. S. Williams, Q. Hu, and J. L. Reno, Appl. Phys. Lett. **88,** 121123 (2006).
9. Y. Sun, B. M. Fischer, and E. Pickwell, J. Biomed. Opt. **14,** 064017 (2009).
10. W. Kan, W. Lee, W. Cheung, V. P. Wallace, and E. Pickwell-MacPherson, Biomed. Opt. Express. **1,** 967 (2010).
11. I. C. Bonzani, J. H. George, and M. Stevens, Current Opn. Chem. Biol. **10,** 568 (2006).